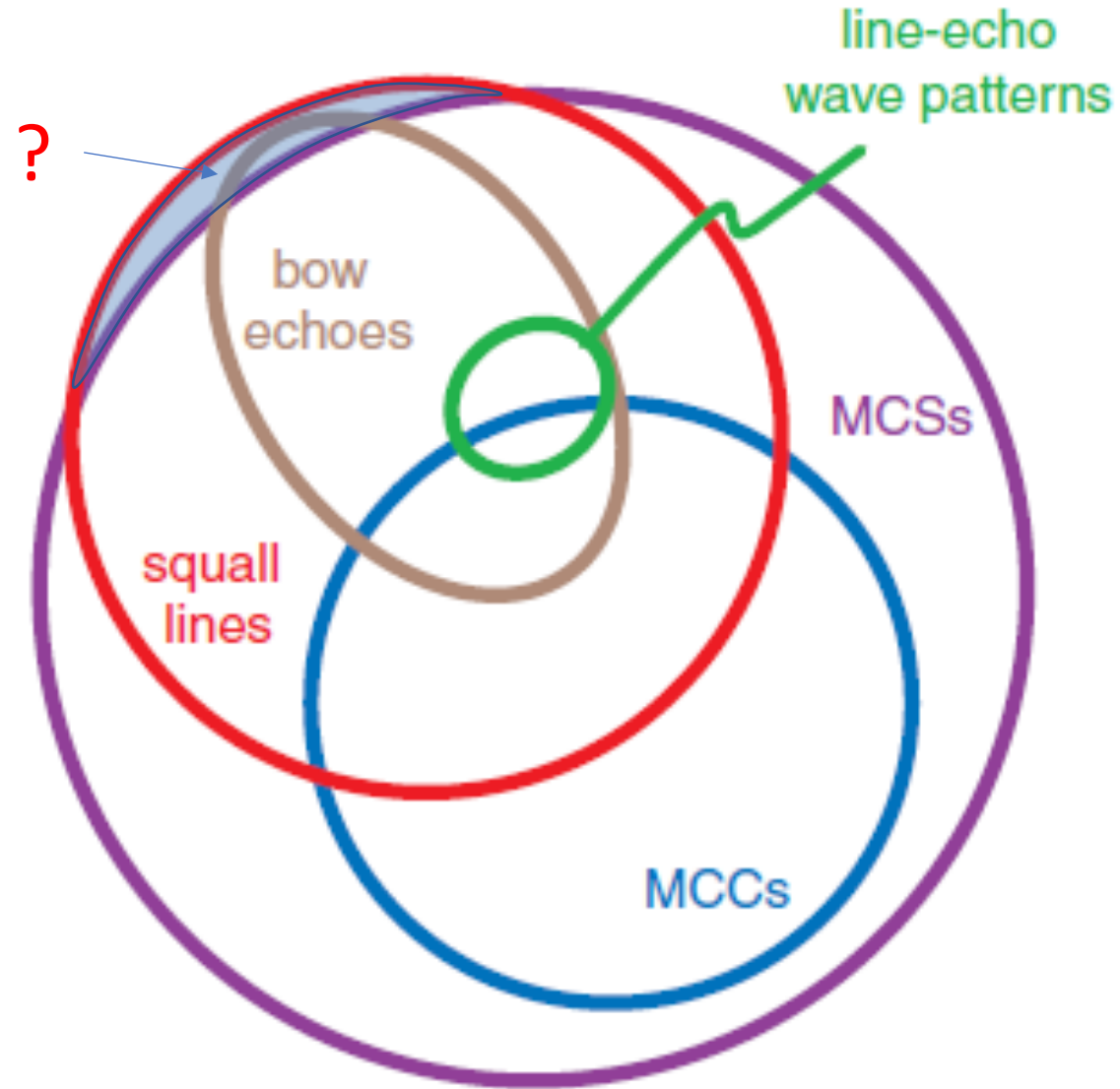


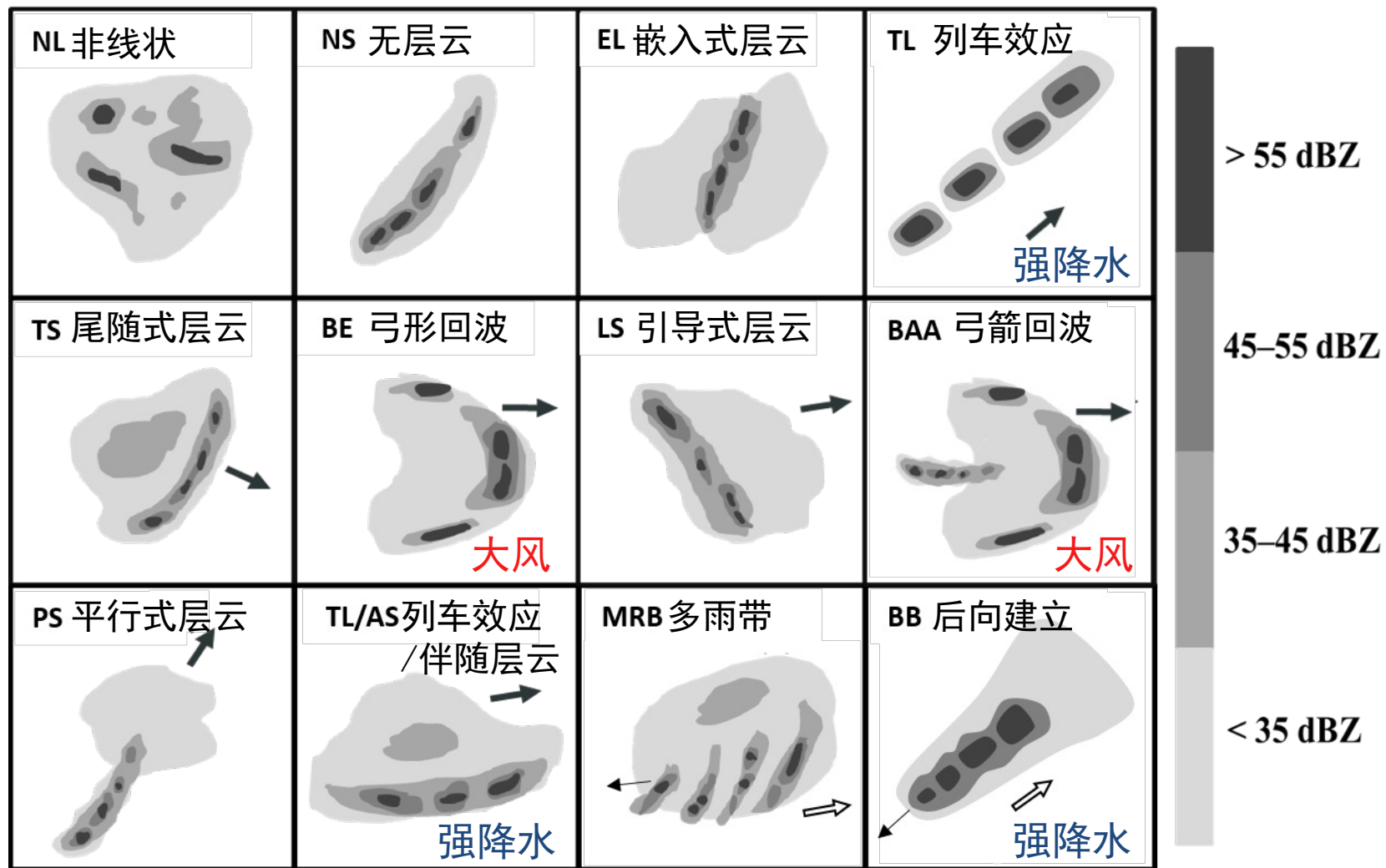
上节课回顾

Relationships among Sub-classifications of MCSs



MCS 的组织形态

上节课回顾

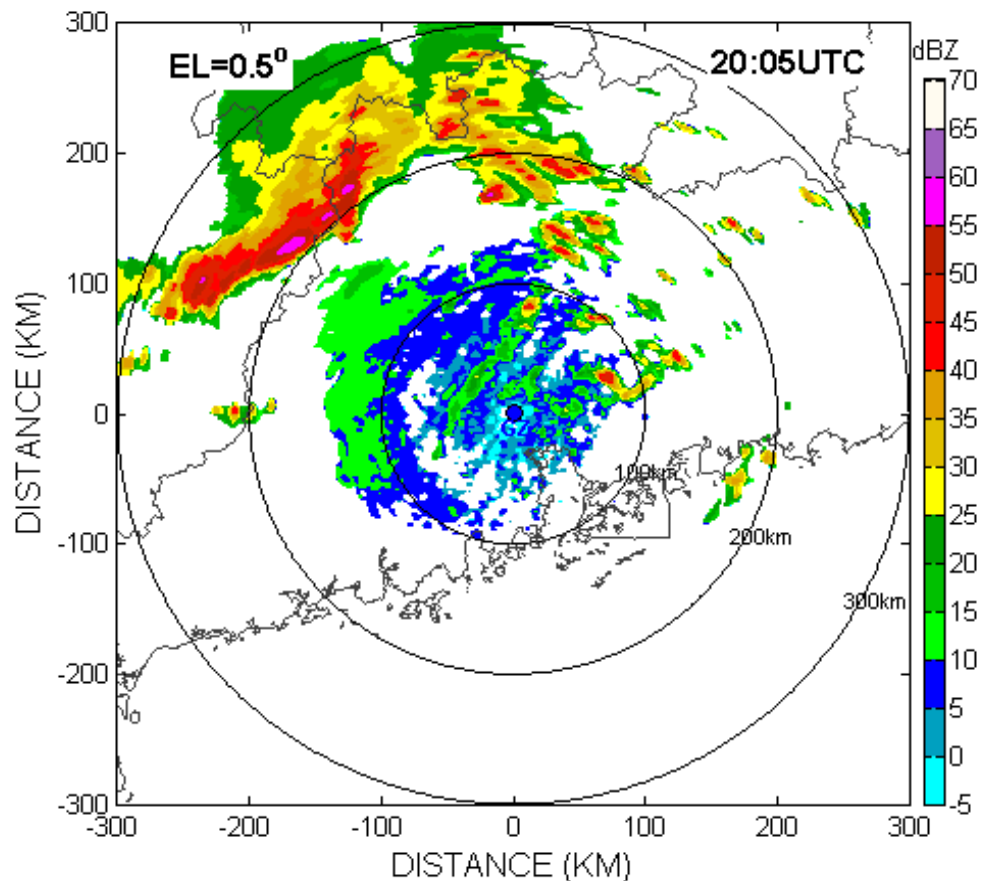


Chappell,1986;Doswell et al., 1996; Schumacher and Johnson,2005;
Keene and Schumacher, 2013; Zheng et al., 2013; Wang Hui et al., 2013

Squall line: structure

上节课回顾

GZ Radar Reflectivity at 0.5 Elevation



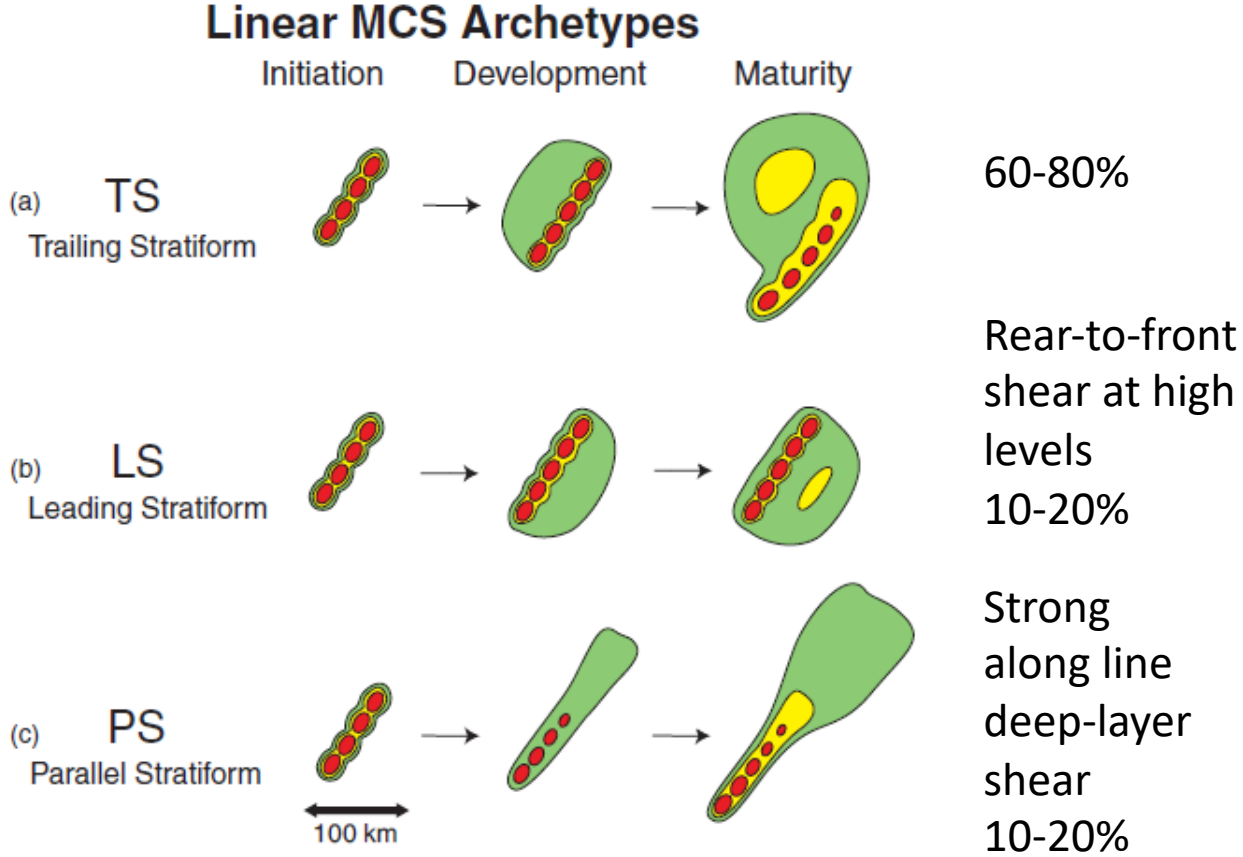
特点: 移速快, 45 km / h,
持续时间长, 约 11 h,
范围广, 横跨广东全省.

灾害: 23日至24日, 广东遭遇
大范围暴雨和雷雨大风
天气, 全省大部分地区
普降强降水。47个市县
出现暴雨, 局部出现大
暴雨, 全省最大降雨量
186.3毫米。曲江的沙溪
镇出现了冰雹。出现了8
级至9级的大风, 花都大
风30米 / 秒 (11级)。

(Zhao kun 2007)

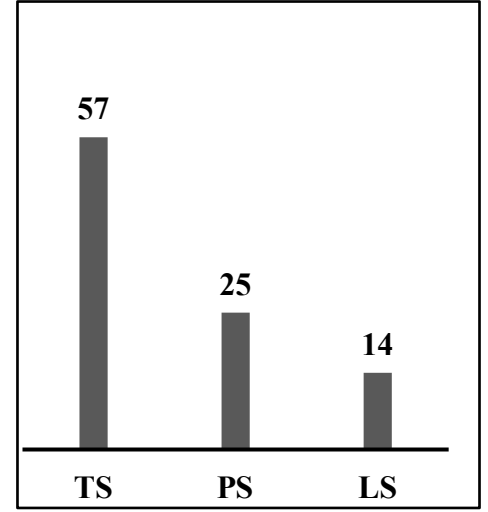
An example of squall line

Squall line organization mode



(Parker and Johnson 2000)

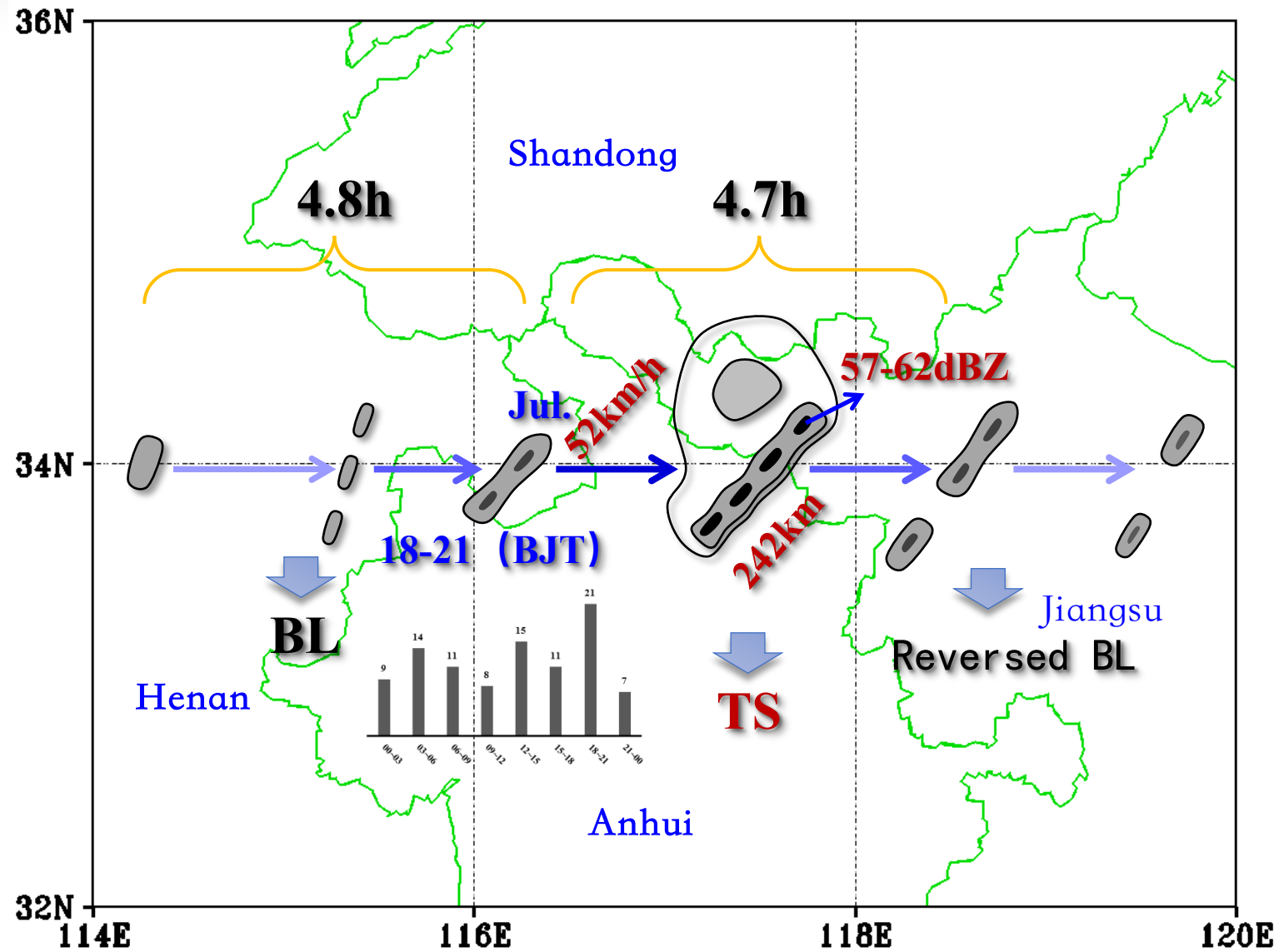
In east China



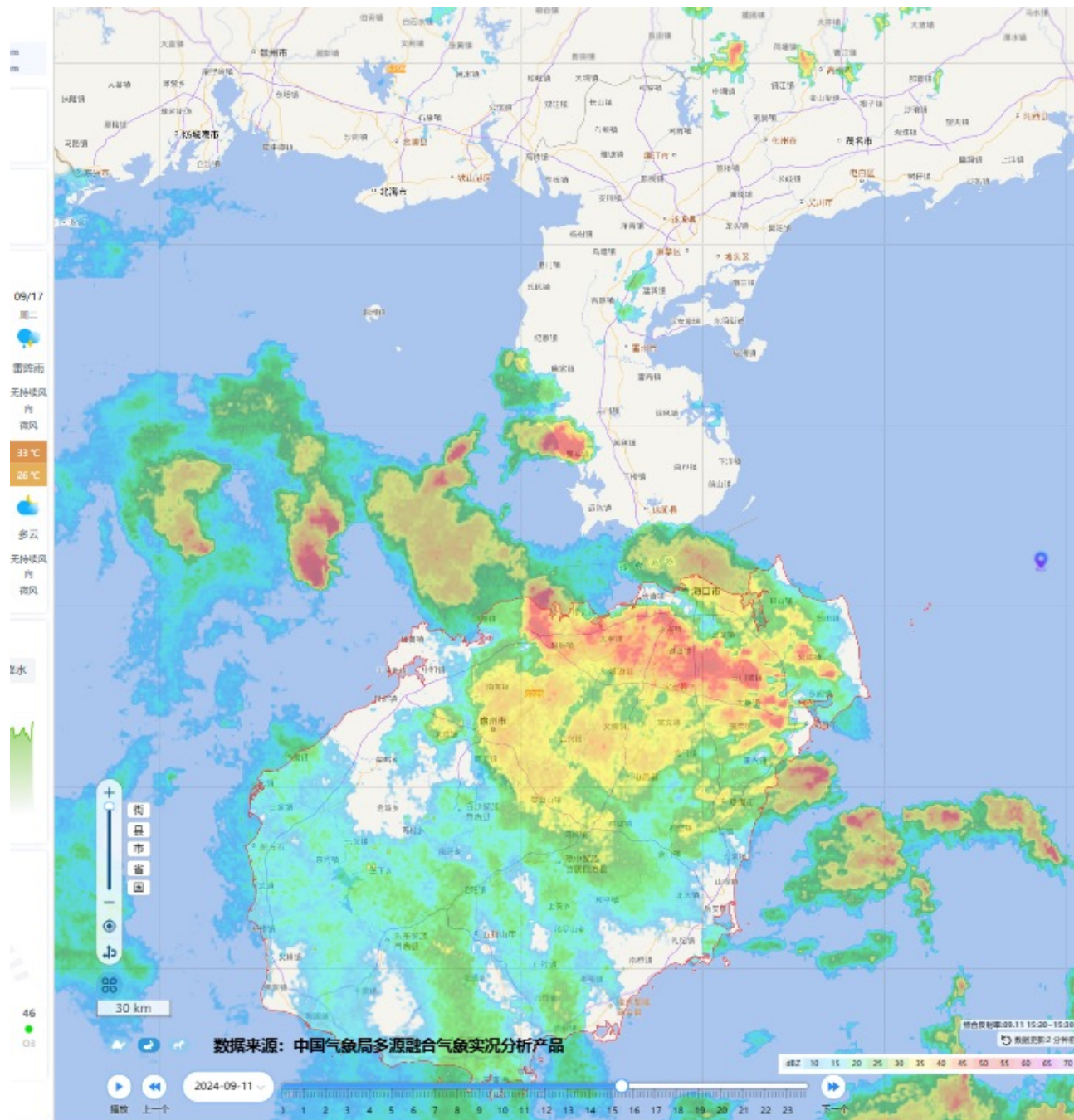
Meng et al. 2013

A Schematic model of squall lines in East China

上节课回顾



更多关于飊线的照片
(感谢孟老师分享!)





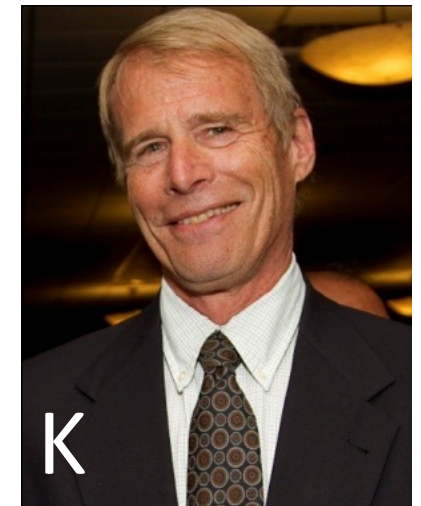
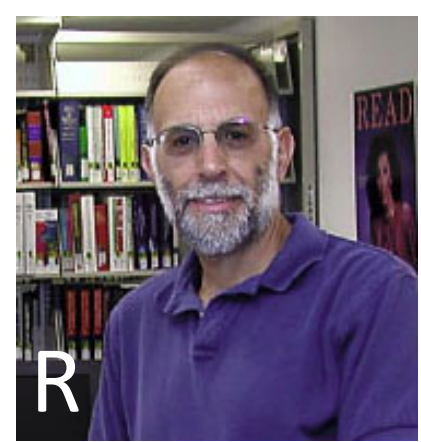
Squall Lines

- Structure
- Formation
- Maintenance
- Rear inflow and bow echoes

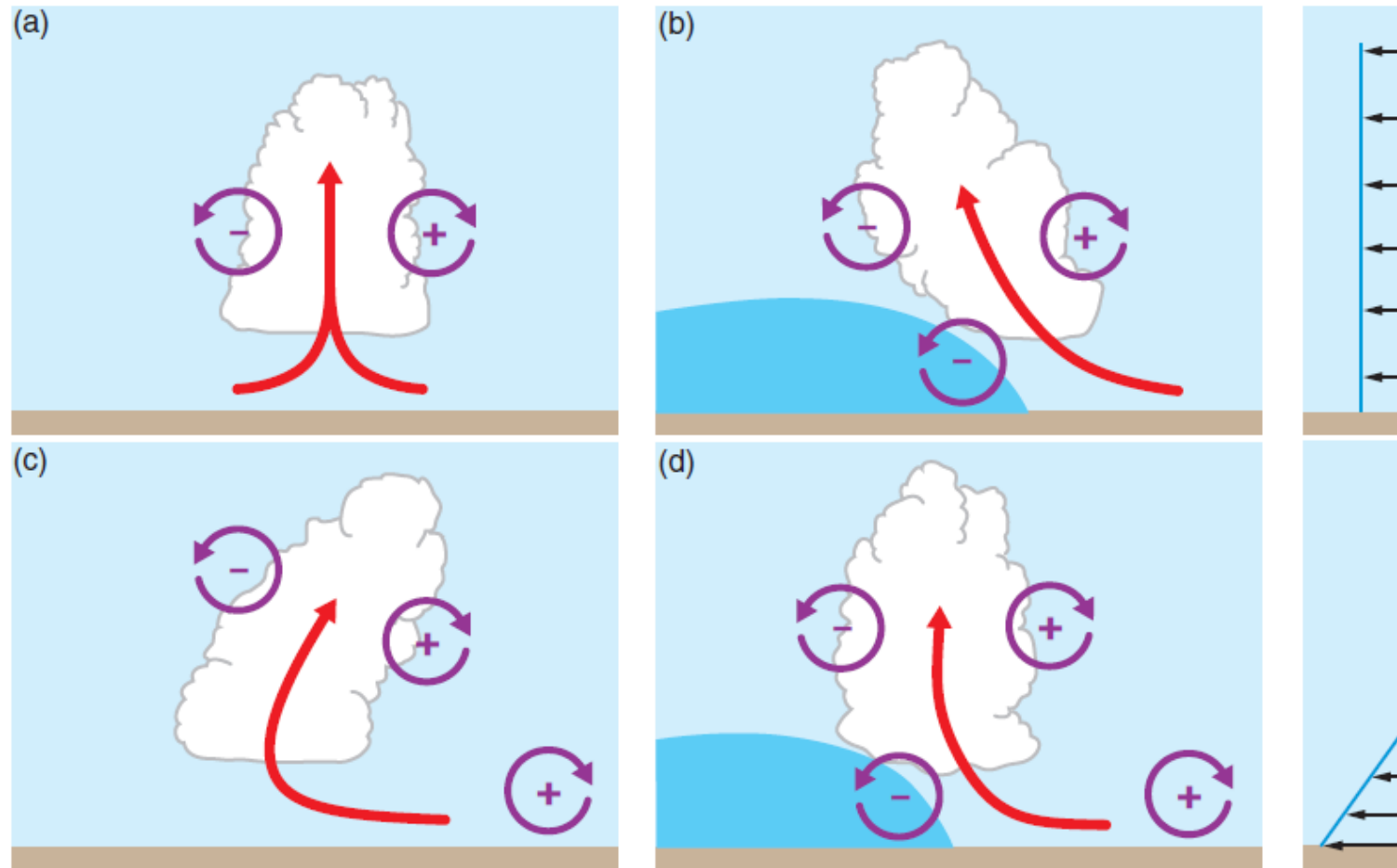
RKW theory

(Rotunno, Klemp, and Weisman 1988)

It postulates that the mechanism for maintaining a long-lived squall line is a balance between the **horizontal vorticity produced by the buoyancy gradient** across the gust front and the **horizontal vorticity associated with the environmental low-level vertical shear**.



RKW theory



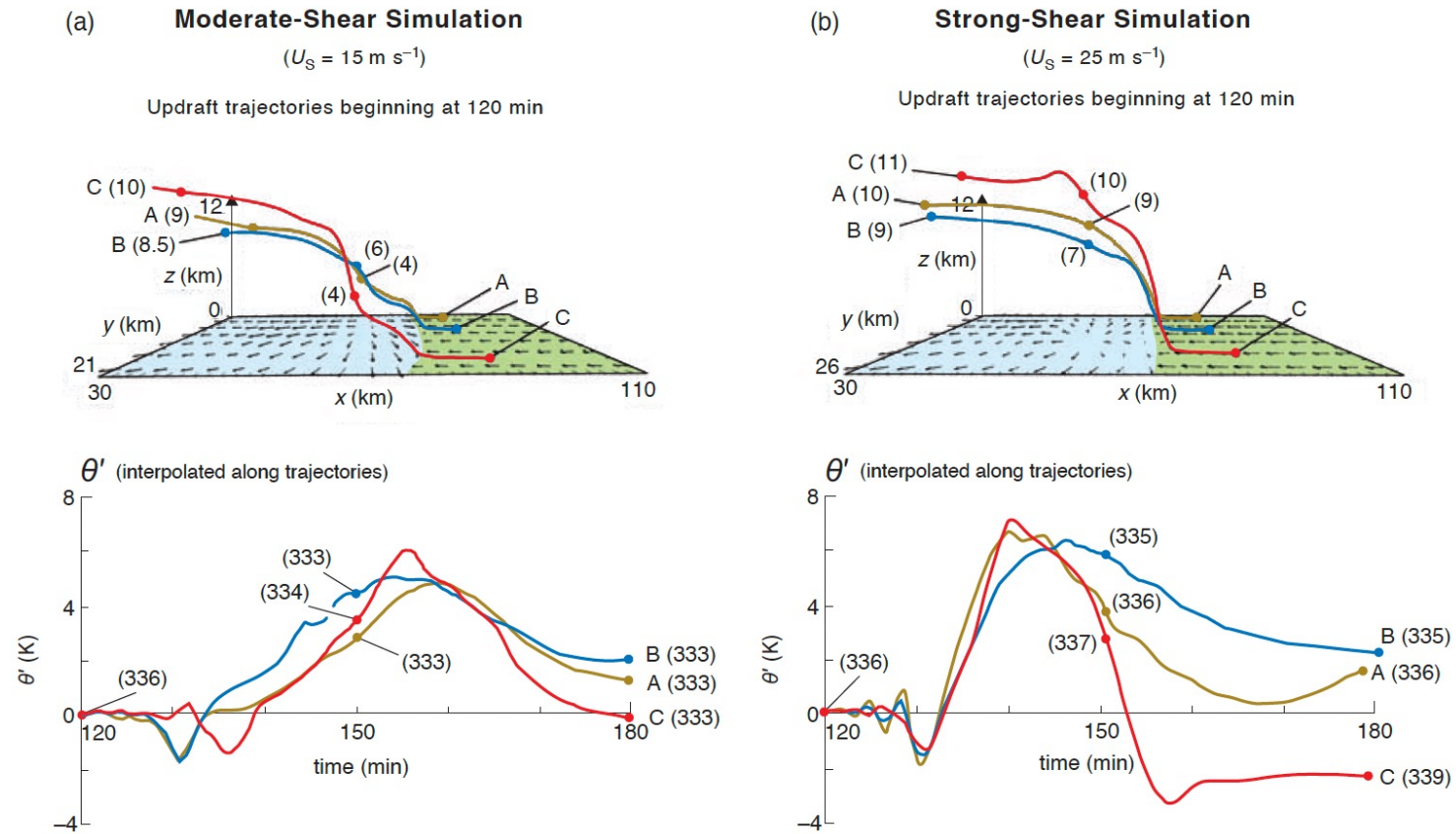


Figure 9.15 Characteristic updraft trajectories and potential temperature perturbations along the trajectories in numerical simulations of a squall line in (a) moderate (15 m s^{-1}) low-level wind shear and (b) strong (25 m s^{-1}) low-level wind shear. Each trajectory originates at 350 m above the surface and about 10 km ahead of the cold pool (blue shading) and is traced for 60 min. The height of each trajectory is indicated in parentheses at 30-min intervals. Numerals in parentheses at 30-min intervals along the potential temperature perturbation traces indicate potential temperatures. Note how the trajectories are more steeply sloped in the strong-shear simulation than in the moderate-shear simulation, and that less buoyancy dilution has occurred along the trajectories in the strong-shear simulation compared with the moderate-shear simulation. (Adapted from Weisman [1992].)

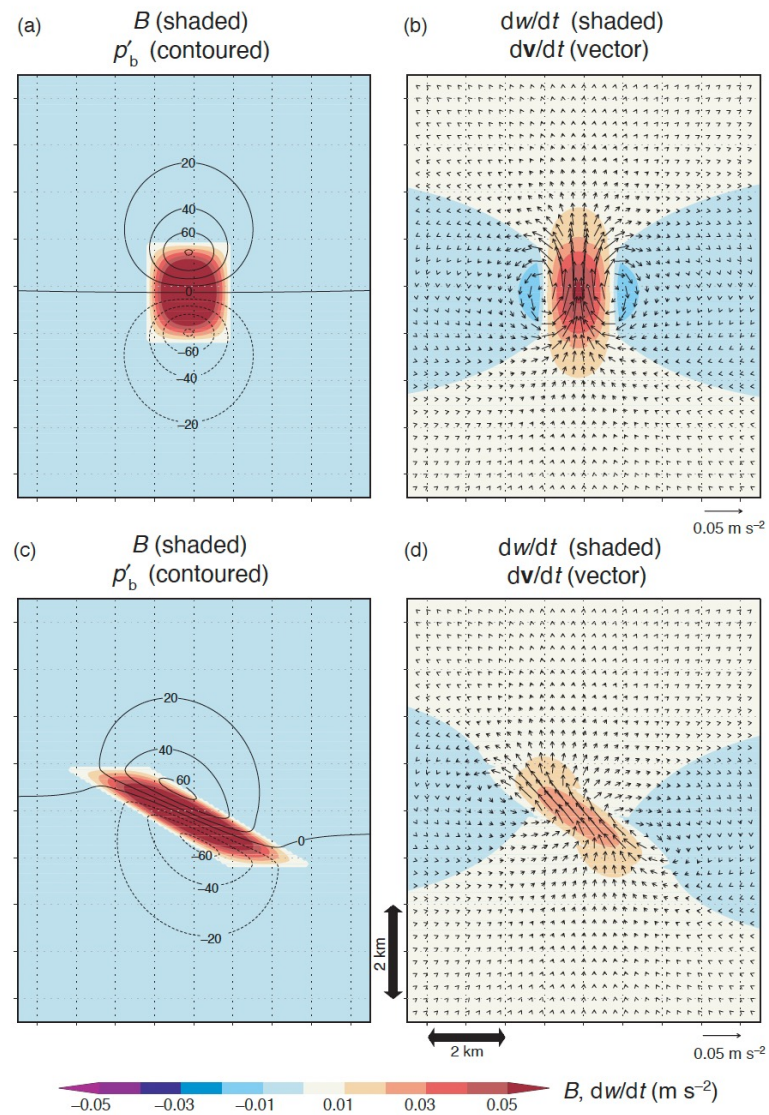


Figure 9.16 The relationship among the tilt of a buoyant column, the buoyancy perturbation pressure field (p'_b), vertical acceleration (dw/dt), and total acceleration ($d\mathbf{v}/dt$). (a) Buoyancy (shaded) and buoyancy perturbation pressure (contours every 20 Pa) fields associated with an upright column of warm air. (b) Vertical acceleration (shaded) and total acceleration (vectors) for the buoyant column shown in (a). (c), (d) As in (a), (b), but the region of positive buoyancy is tilted. The maximum buoyancy in (c) is the same as in (a), but the downward-directed gradient of p'_b is larger within the buoyant column, resulting in a smaller vertical acceleration in (d) compared with (b). Courtesy of Matt Parker.

Density current in a control volume

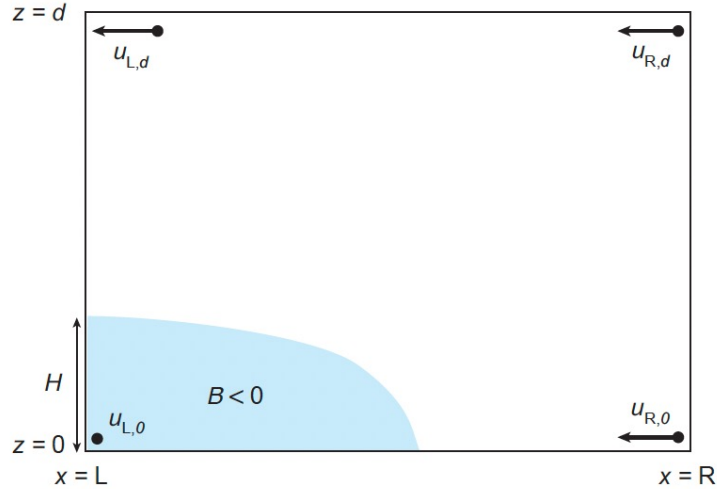


Figure 5.29 Schematic of the relationship between a density current and the control volume described in the text. All winds are relative to the density current.

$$\frac{d\eta}{dt} = -\frac{\partial B}{\partial x},$$

$$\frac{\partial \eta}{\partial t} = -\frac{\partial(u\eta)}{\partial x} - \frac{\partial(w\eta)}{\partial z} - \frac{\partial B}{\partial x}.$$

$$\begin{aligned} \frac{\partial}{\partial t} \int_0^d \int_L^R \eta \, dx \, dz &= - \int_0^d \int_L^R \frac{\partial(u\eta)}{\partial x} \, dx \, dz \\ &\quad - \int_L^R \int_0^d \frac{\partial(w\eta)}{\partial z} \, dz \, dx \\ &\quad - \int_0^d \int_L^R \frac{\partial B}{\partial x} \, dx \, dz \end{aligned} \quad (5.37)$$

$$\begin{aligned} &= - \int_0^d [(u\eta)_R - (u\eta)_L] \, dz \\ &\quad - \int_L^R [(w\eta)_d - (w\eta)_0] \, dx \\ &\quad - \int_0^d (B_R - B_L) \, dz. \end{aligned} \quad (5.38)$$

详细推导见板书!

$$0 = \int_0^d u_L \, du_L - \int_0^d u_R \, du_R - \int_L^R (w\eta)_d \, dx + \int_0^H B_L \, dz \quad (5.40)$$

$$\begin{aligned} &= \left(\frac{u_{L,d}^2}{2} - \frac{u_{L,0}^2}{2} \right) - \left(\frac{u_{R,d}^2}{2} - \frac{u_{R,0}^2}{2} \right) - \int_L^R (w\eta)_d \, dx \\ &\quad + \int_0^H B_L \, dz, \end{aligned} \quad (5.41)$$

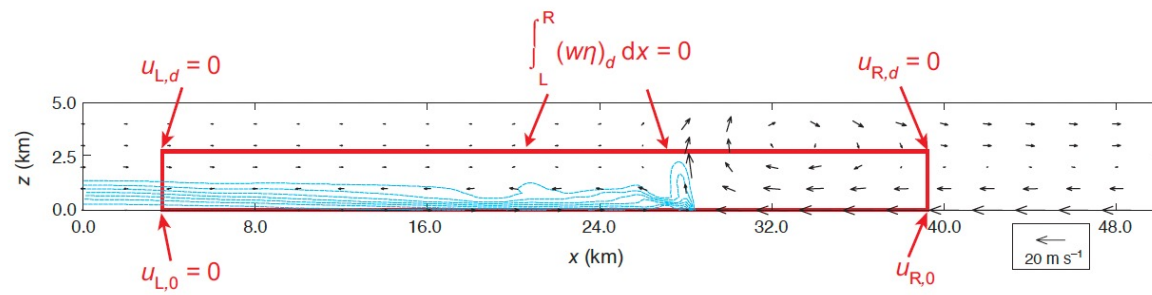


Figure 9.17 Numerical simulation of an eastward-moving density current in an environment containing westerly vertical wind shear such that the circulation associated with the environmental shear approximately balances the circulation associated with the density current (i.e., the environment approximately satisfies RKW theory's optimal state). The result is an erect updraft along the leading edge of the density current. The control volume considered in the derivation of the optimal shear is overlaid in red. Potential temperature perturbations are contoured at 1°C intervals within the cold pool starting at -1°C . Wind vectors are relative to the density current ($U_c \approx 8 \text{ m s}^{-1}$). The model domain extends to 10 km; only the lowest 5 km of the model domain are shown.

Setting $u_{L,d} = u_{R,d} = u_{L,0} = \int_L^R (w\eta)_d dx = 0$ in (9.1) yields

$$0 = \frac{u_{R,0}^2}{2} + \int_0^H B_L dz; \quad (9.2)$$

thus,

$$u_{R,0}^2 = -2 \int_0^H B_L dz = c^2 \quad (9.3)$$

$$u_{R,0} = -c, \quad (9.4)$$

where c is the strength of the cold-pool circulation. The reason for taking the negative root in (9.4) will be apparent below. Because $u_{R,d} = 0$, (9.4) can be written as

$$\Delta u = c, \quad (9.5)$$

Optimal condition $\Delta u = c$

- Δu is line-normal vertical shear over 0-2.5km
- C is the theoretical gust front speed, which is the square of twice the integration of buoyancy in the cold pool over the depth of the cold pool.

$$-2 \int_0^H B_L dz = c^2$$

For most thunderstorm outflows, RKW theory implies an optimal shear of 17-25 m/s over 0-2.5km layer.

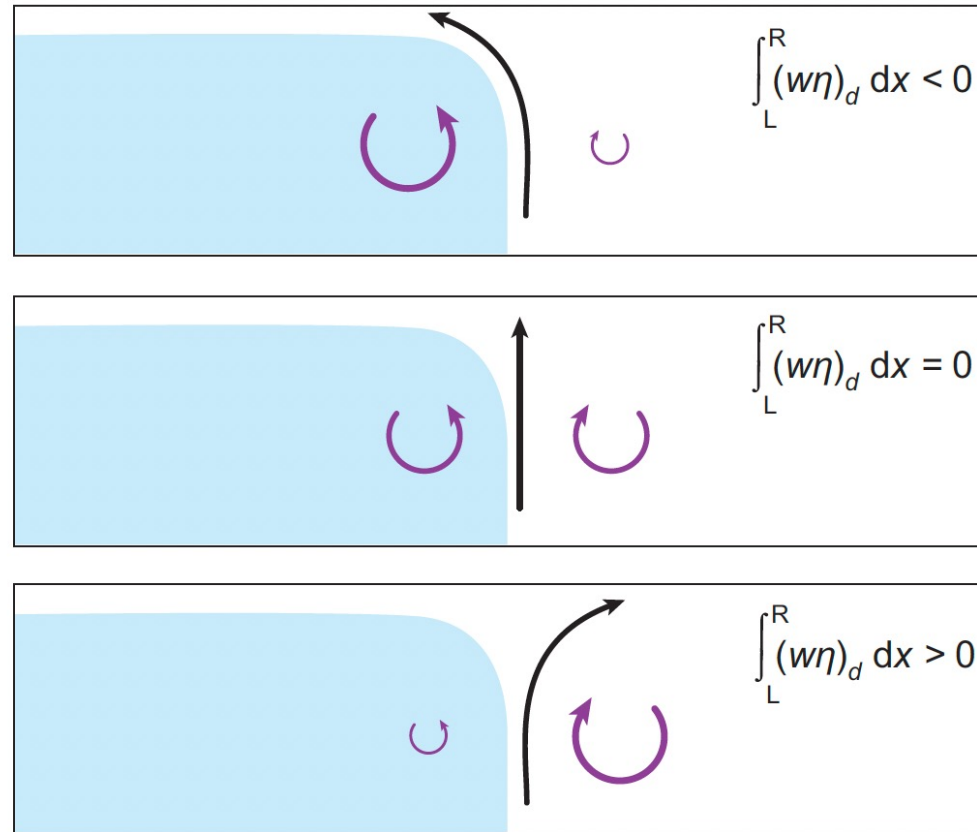


Figure 9.18 Schematic showing the relationships between the net flux of horizontal vorticity through the top of the control volume, $\int_L^R (w\eta)_d dx$, and updraft tilt. (a) The cold-pool horizontal vorticity (defined to be negative) dominates the horizontal vorticity associated with the mean low-level shear (defined to be positive); air lifted by the cold pool is accelerated rearward and exits the top of the control volume at an angle, and there is a net flux of negative vorticity through the top of the volume. (b) The cold-pool horizontal vorticity balances the horizontal vorticity associated with the mean low-level shear; the updraft at the leading edge of the cold pool is not tilted and there is no net flux of vorticity through the top of the volume. (c) The horizontal vorticity associated with the mean low-level shear dominates the cold-pool horizontal vorticity; air lifted by the cold pool is accelerated forward and exits the top of the control volume at an angle, and there is a net flux of positive vorticity through the top of the volume.

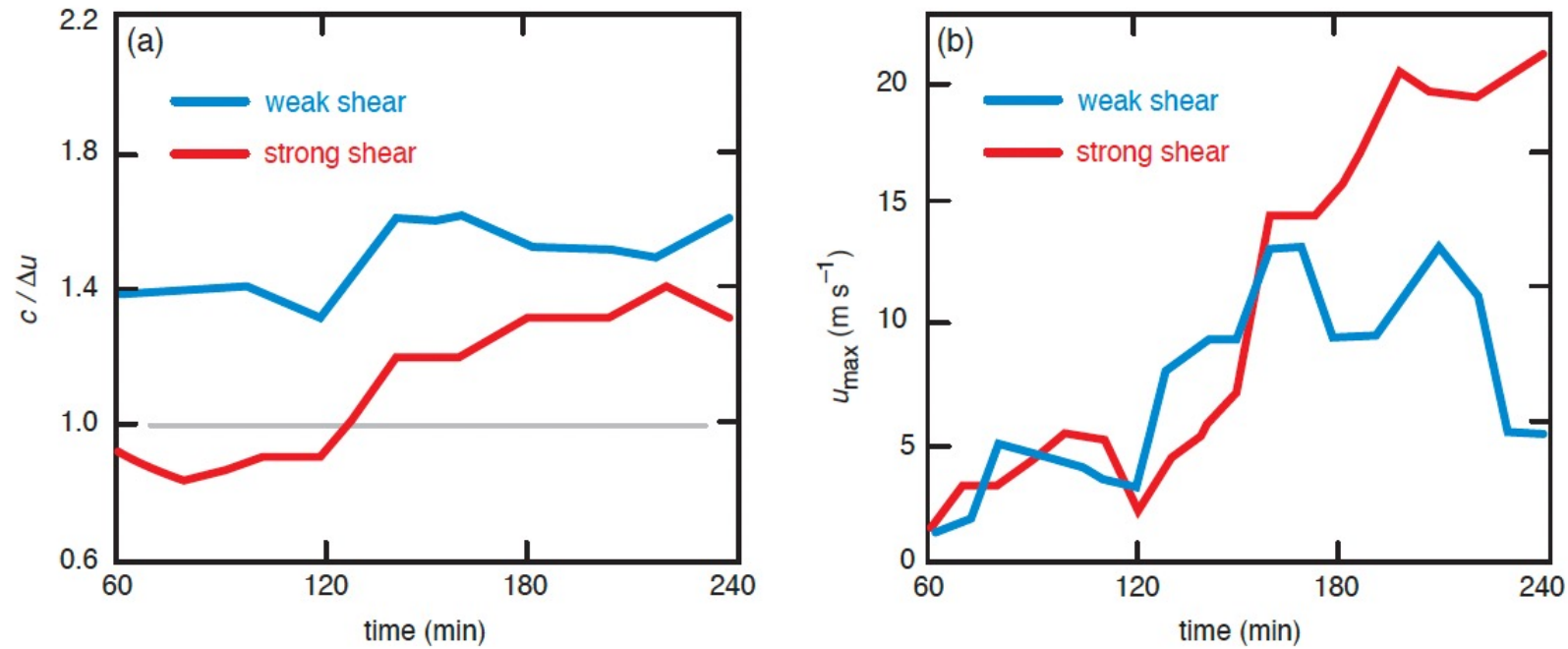
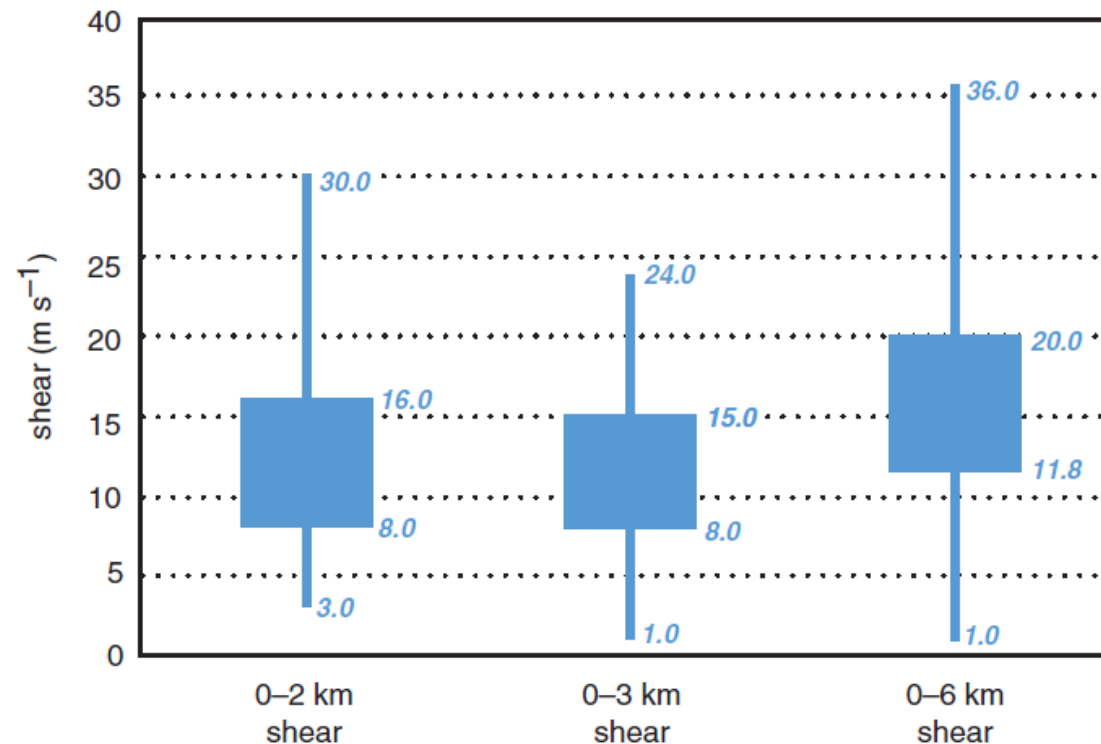


Figure 9.19 Time series of (a) $c/\Delta u$ and (b) maximum midlevel rear inflow strength in a pair of numerical simulations of squall lines in which the environment has relatively weak (15 m s^{-1}) low-level wind shear and relatively strong (25 m s^{-1}) low-level wind shear. (Adapted from Weisman [1992].)

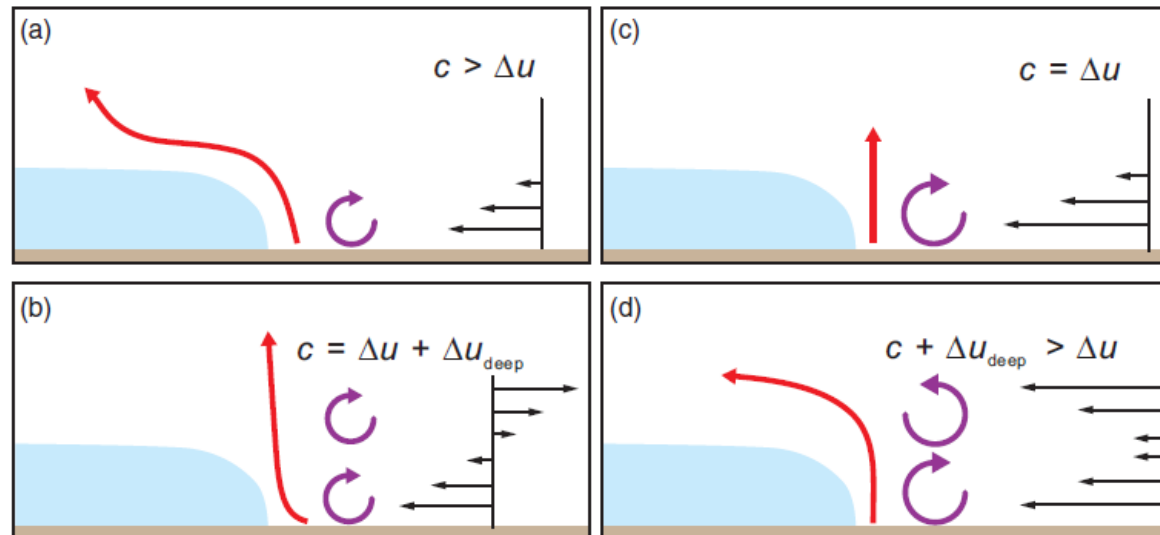
Controversy about RKW theory

- **Shear vs. Severity** : the vertical shear is significantly weaker than required by RKW for many **strong-wind producing** squall lines



Possibilities

1. The **optimal condition needs not to be met** in order for severe weather to occur
2. The appearance of **straight-line winds** in a squall line is not a reliable indication for the **erect updraft**.
Obs shows that **upshear-tilted updraft** tends to have bow echoes and strong surface winds
3. Mid and upper tropospheric vertical wind shear is also very important.



It is Likely

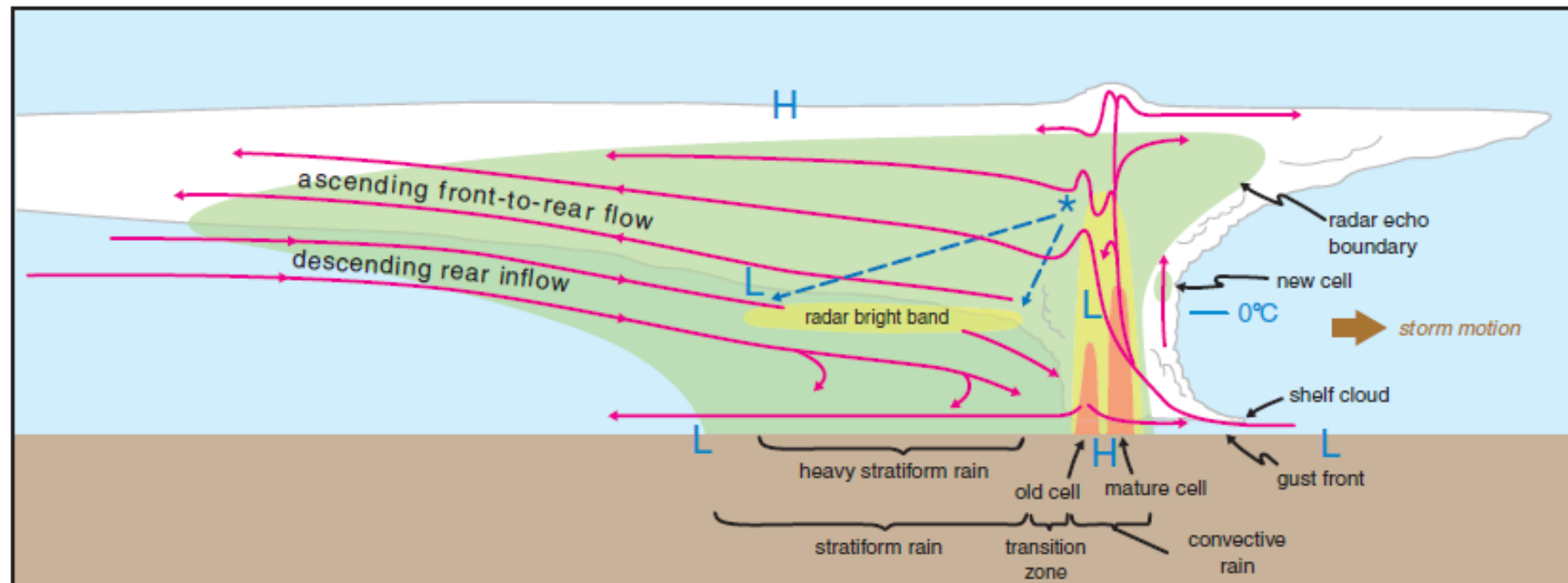
- RKW theory **overstates** the importance of the upright of the **gust front updraft** in attempting to explain squall line longevity.
 - It became irrelevant if the top of the cold pool is higher than LFC
- More applicable to the issue of **convection initiation** than convection maintenance

Squall Lines

- Structure
- Formation
- Maintenance
- Rear inflow and bow echoes

General features of Rear Inflow (RI)

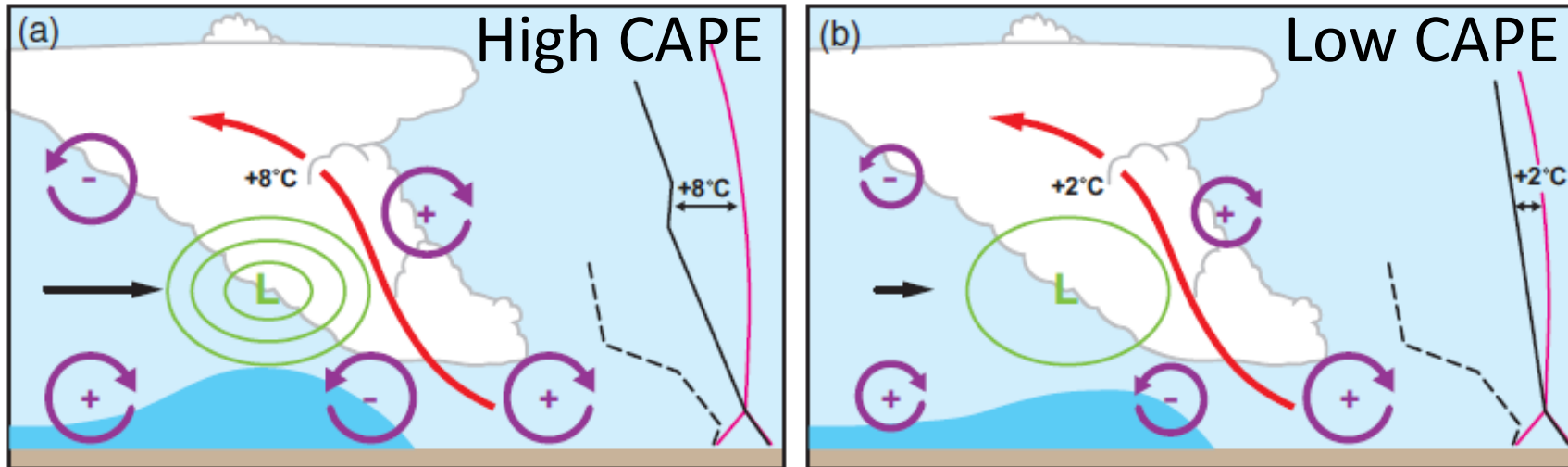
- A very common trait for TS squall line
- RI happens when the updrafts tilt rearward over their cold pools.



RI: formation

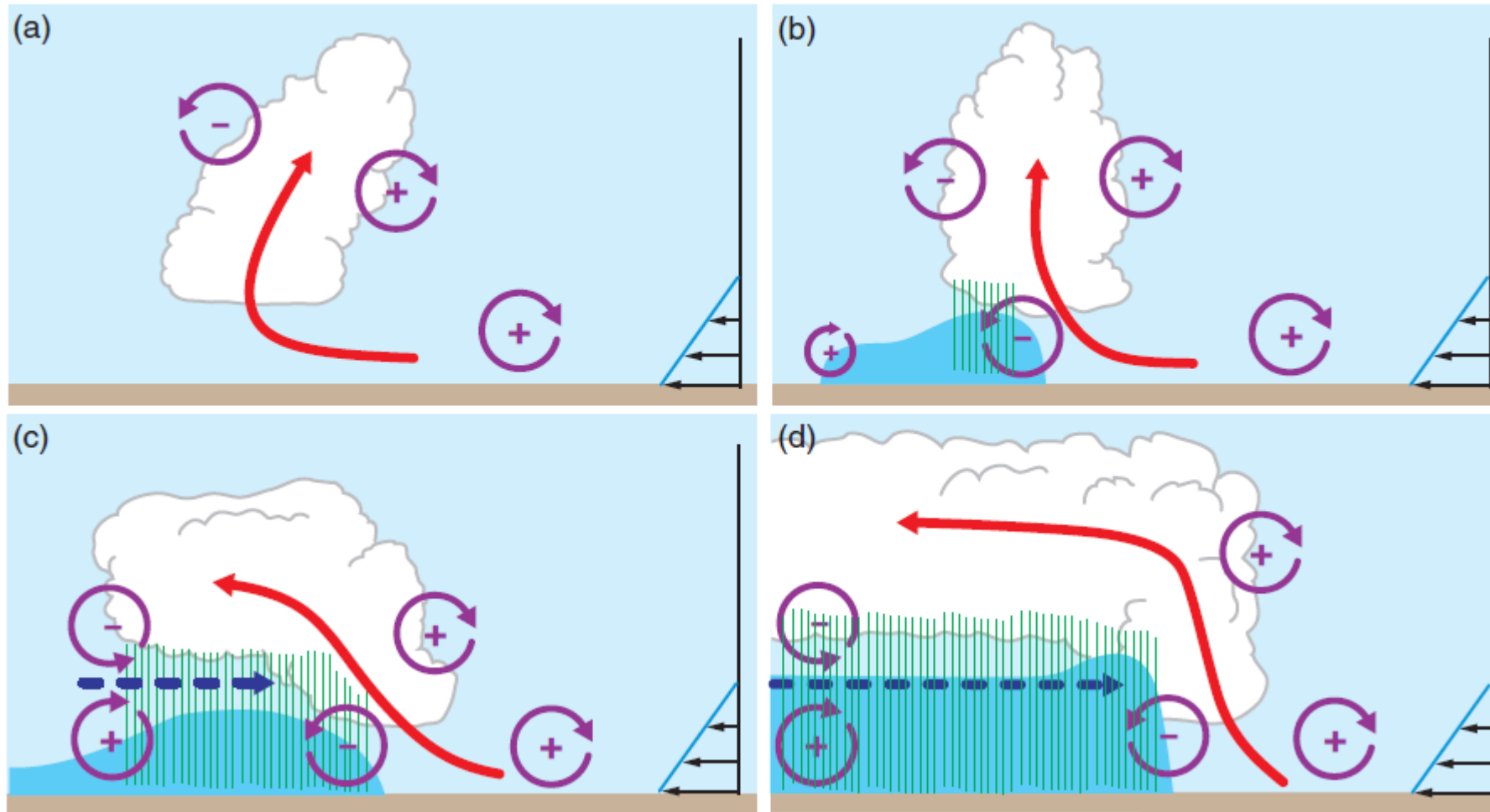
Aspect 1: Mid-level pressure deficit
as a result of $\partial B/\partial z > 0$

$$p' \propto \underbrace{\left[\left(\frac{\partial u'}{\partial x} \right)^2 + \left(\frac{\partial v'}{\partial y} \right)^2 + \left(\frac{\partial w'}{\partial z} \right)^2 \right]}_{\text{fluid extension terms}} \underbrace{-\frac{1}{2} \zeta'^2}_{\text{spin term}} + \underbrace{2\mathbf{S} \cdot \nabla_h w'}_{\text{linear dynamic pressure perturbation, } p'_{dl}} - \underbrace{\frac{\partial B}{\partial z}}_{\text{buoyancy pressure perturbation, } p'_b} \quad (8.24)$$



Aspect 2: Vorticity couplets at the rear of the cold pool

RI impact on the updraft



$$\Delta u^2 + \Delta u_j^2 = c^2,$$

Bow Echo

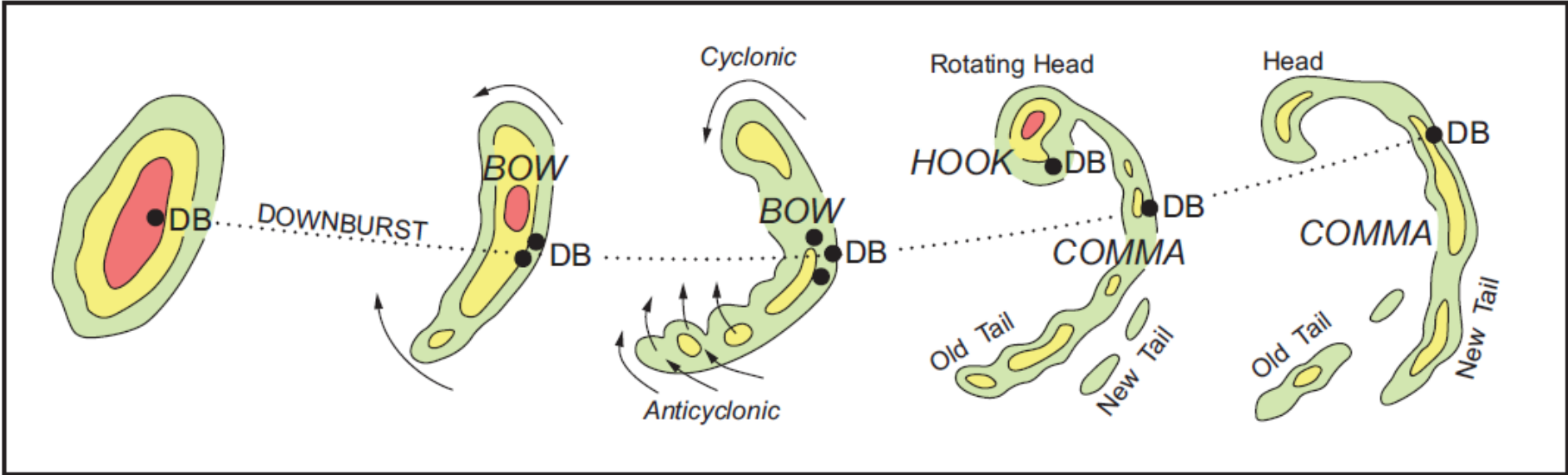


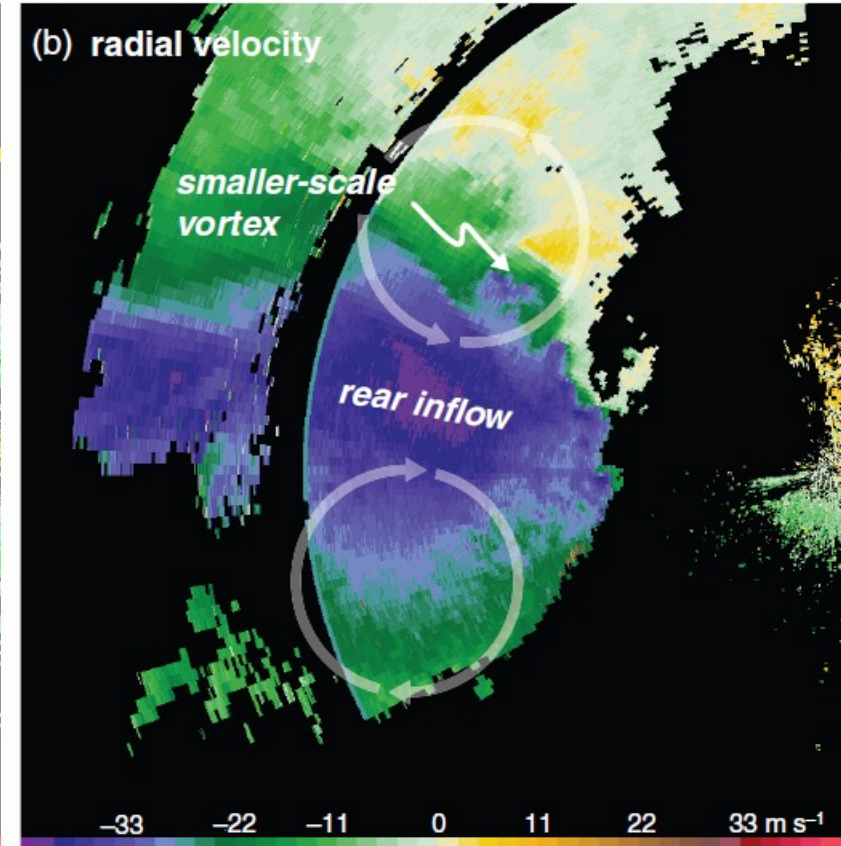
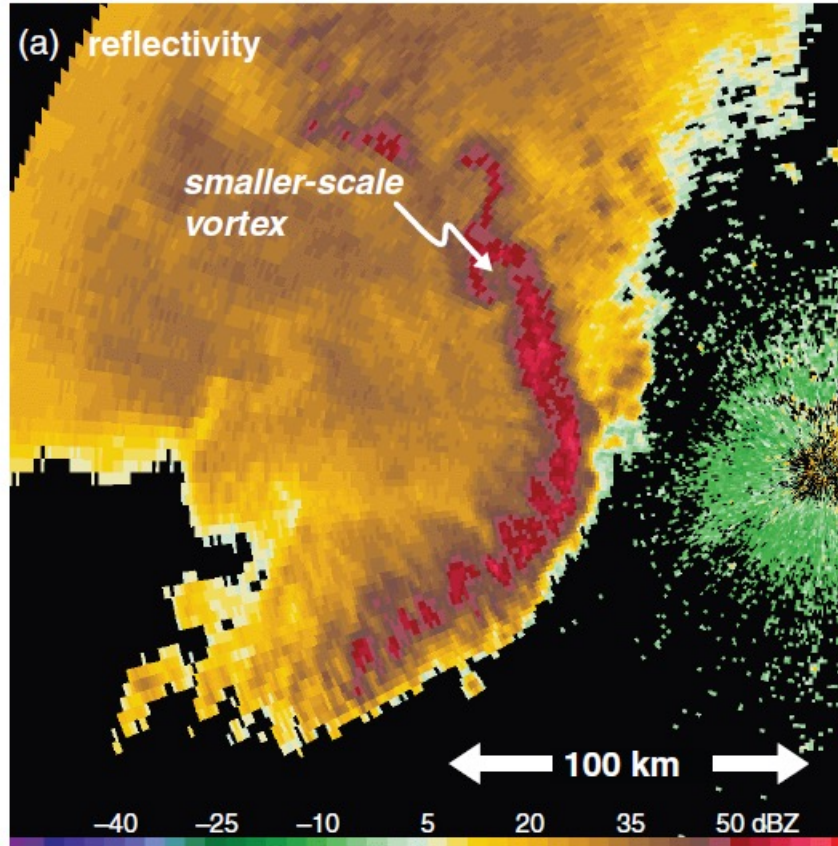
Figure 9.24 Fujita's conceptual model of a bow echo. Black dots labeled 'DB' are downburst locations. Colors are radar echo intensity. (Adapted from Fujita [1978].)

Rear inflow

Line-end vortices Bookend vortices

Bow echo: example

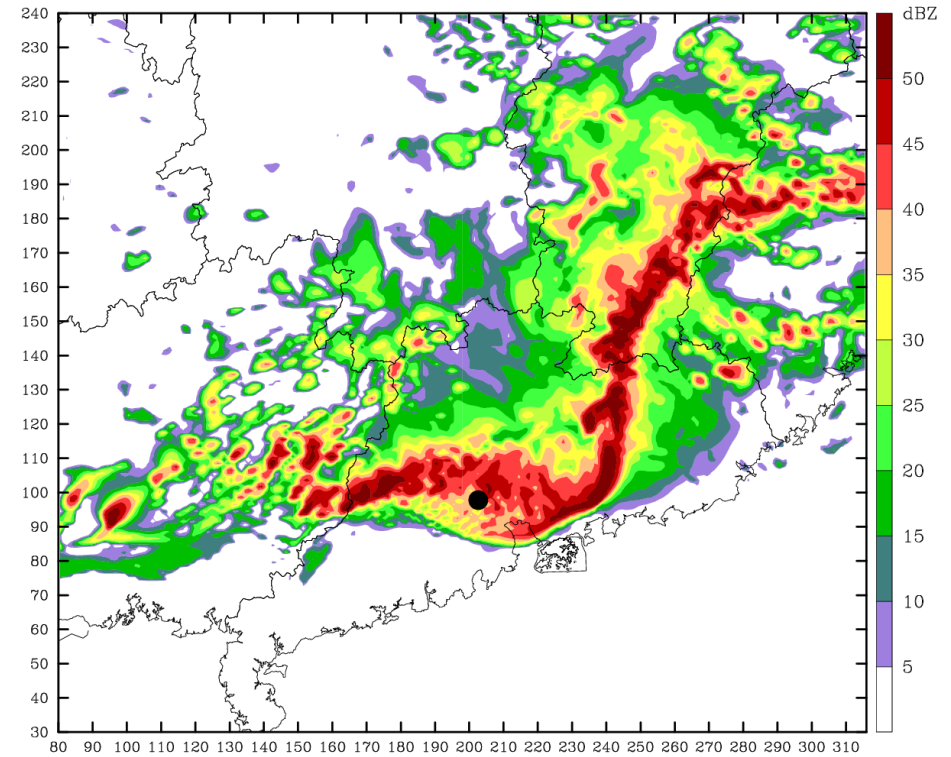
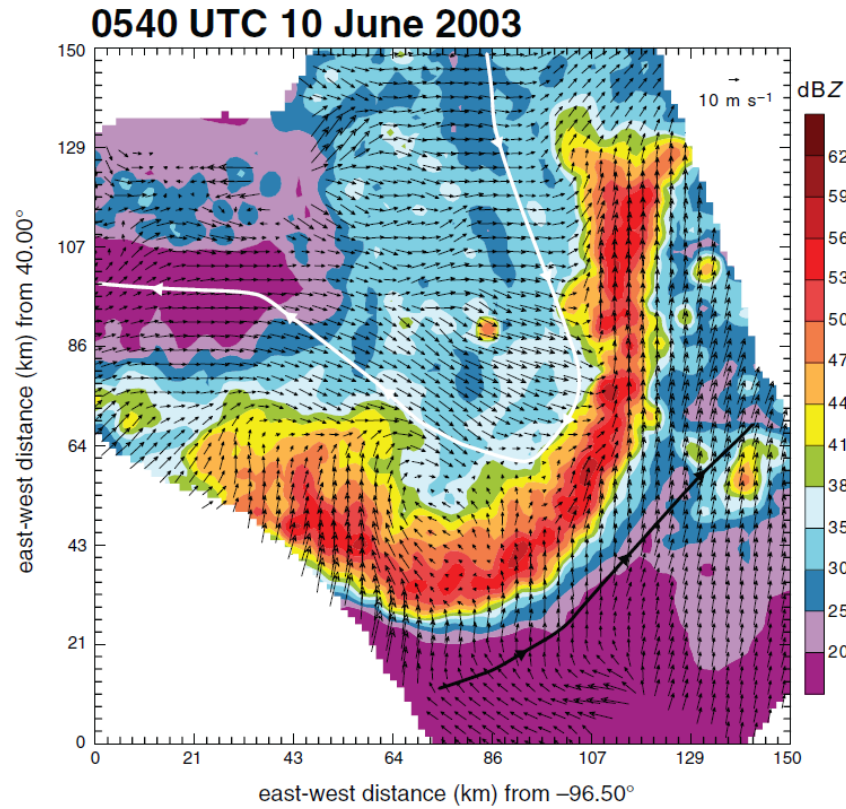
1848 UTC 5 May 1996



Bow echo: other cases

CTRL-PERT: Temp. difference
Fcst: 12.00 h
Max Reflectivity ()

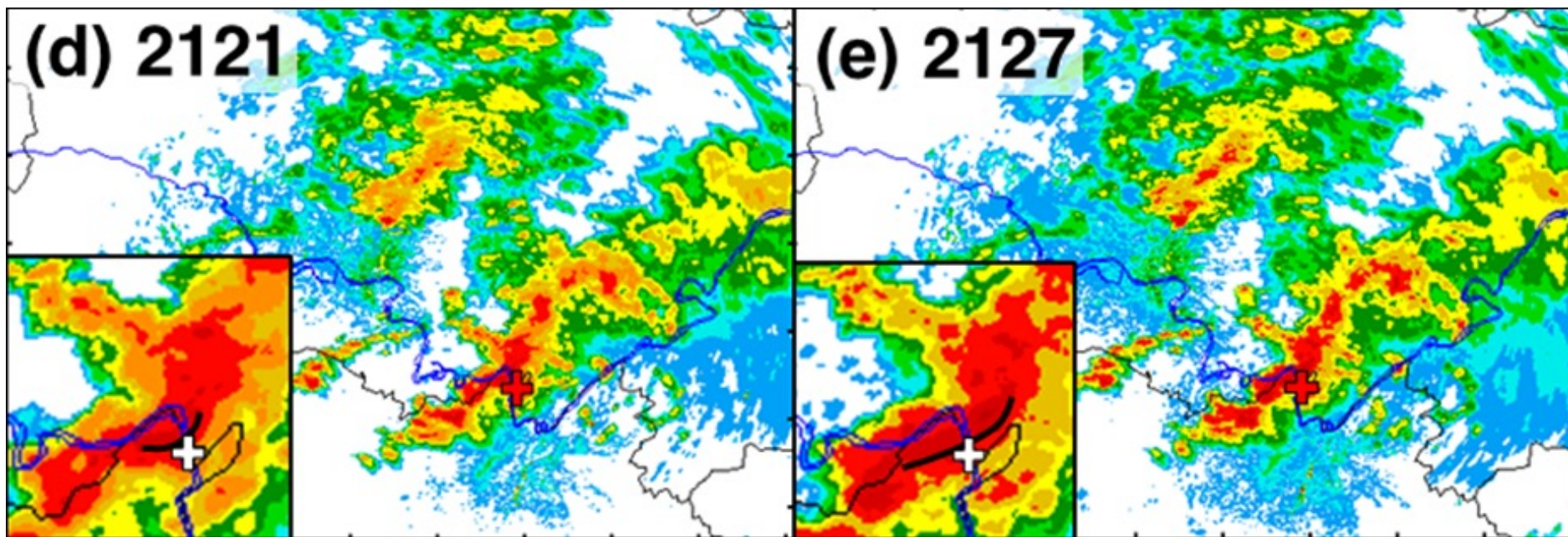
Init: 1200 UTC Mon 23 Apr 07
Valid: 0000 UTC Tue 24 Apr 07 (1800 MDT Mon 23 Apr 07)



Model Info: V2.2.1 No Cu YSU PBL WSM 6class Ther-Diff 4.5 km, 34 levels, 20 sec
LW: RRTM SW: Dudhia DIFF: simple KM: 2D Smagor

Bow echo: other cases

2015.6.1 东方之星



Bow echo: general features

- Size: 20-200 km long
- **Damaging winds** usually appears at the **apex**, especially when the **RIJ** descends to the surface.
- Large CAPE and Larger low-level shear
 - Severe damaging cases with CAPE > 5000 j/kg,
0-2 km shear ~25 m/s.

Why such a strong shear is needed?

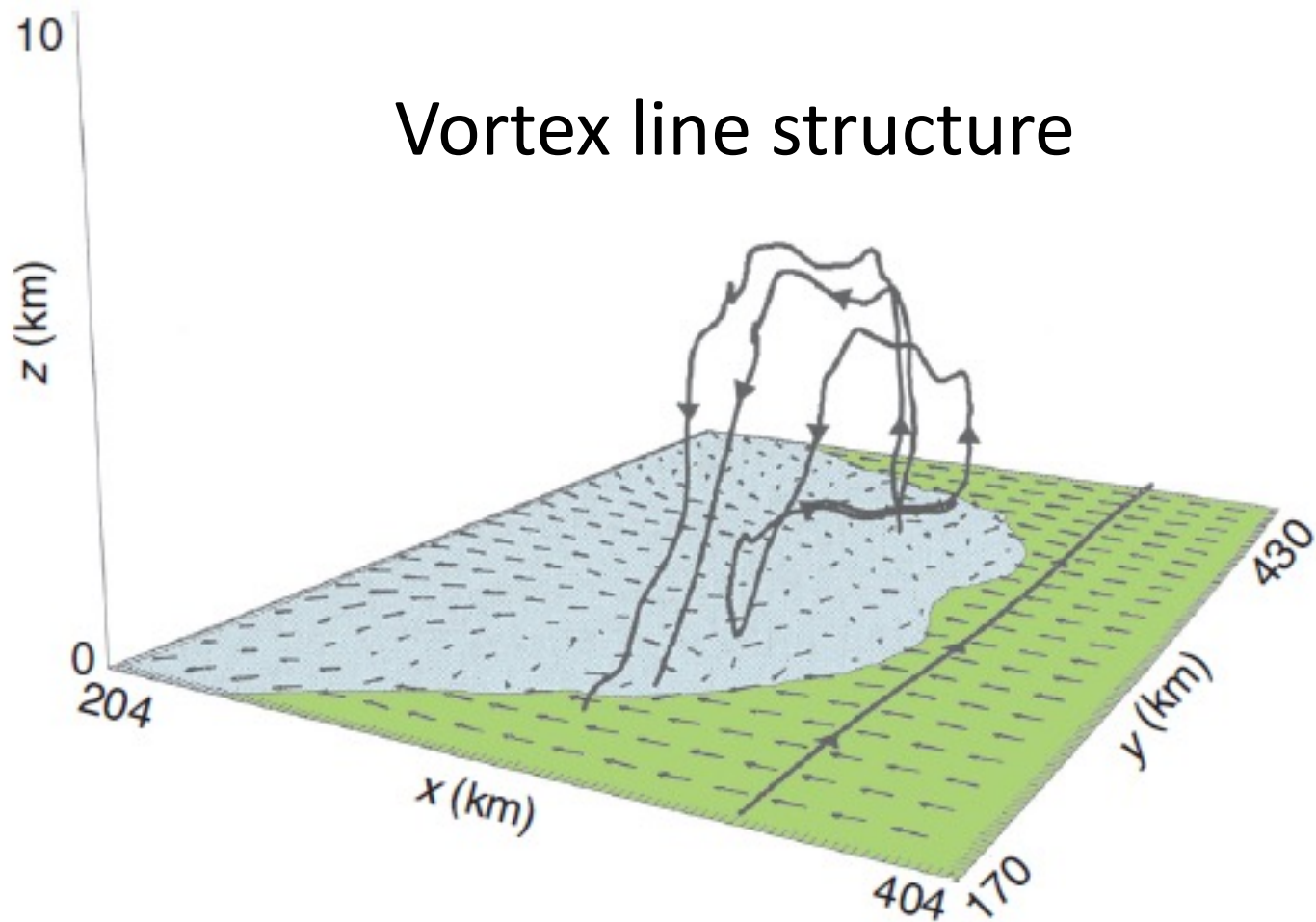
- Create a preferred zone of **lifting** , leading to a focused area of updraft necessary for tilting
- Balance the usually strong cold pool associated with the large CAPE
- Create an erect updraft → less entrainment → less reduction to the buoyancy → **larger mid-level pressure deficit** when it is finally tilted rearward

Bow echo or Supercell?

- Bow echo can evolve from supercell esp. HP supercell.
- Whether **a bow echo** or **a supercell** develop in a strong shear environment lies in subtleties of
 - Initiation mechanism
 - Cell interactions
 - Details of the environment (vertical distribution of CAPE and shear, mid-level RH).

The RH change associated with **several g/kg** change of mixing ratio are sufficient to go from the slab to cellular regime.

Formation of line End Vortices:



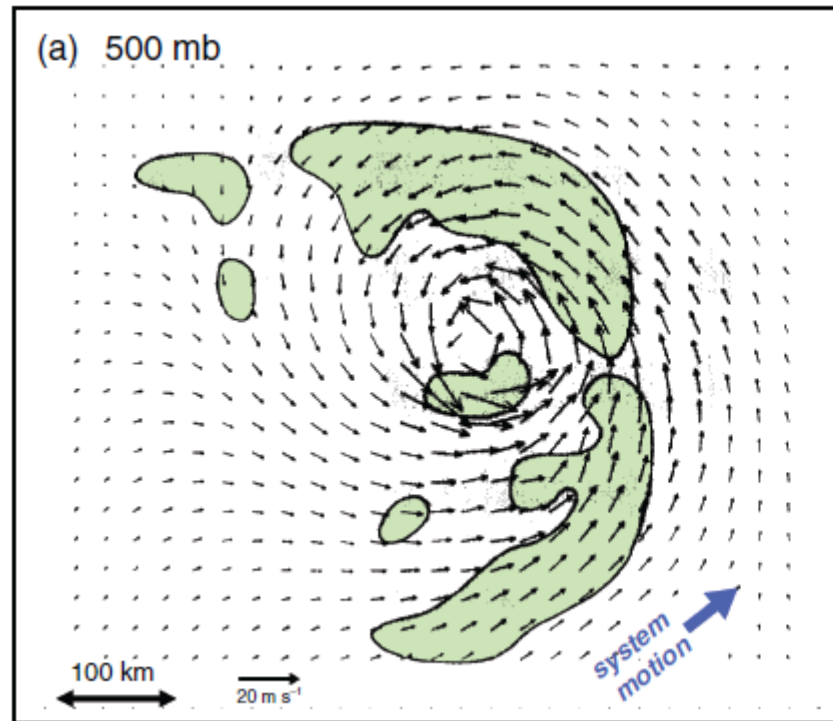
Mesoscale Convective Complexes

General features

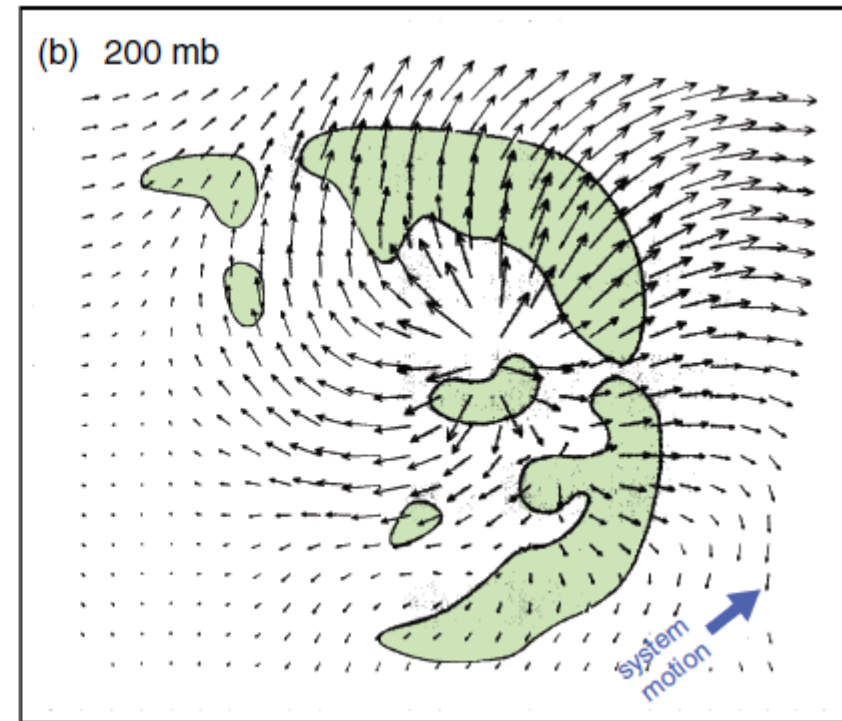
- A large, circular, long-lived, cold **cloud** shields
- Many squall lines and bow echo can be classified as MCCs
- Greater **nocturnal bias** than MCSs in general
- **Slow movement** with high flash flood threat

Structure

MCCs generate warm core meso- α -scale circulation

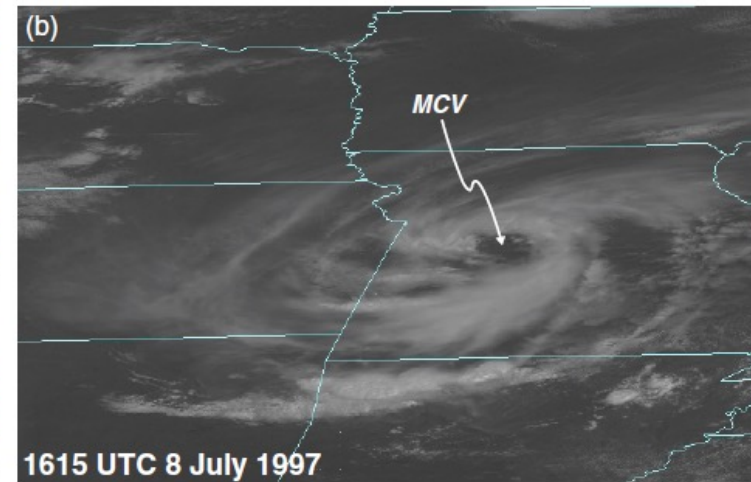
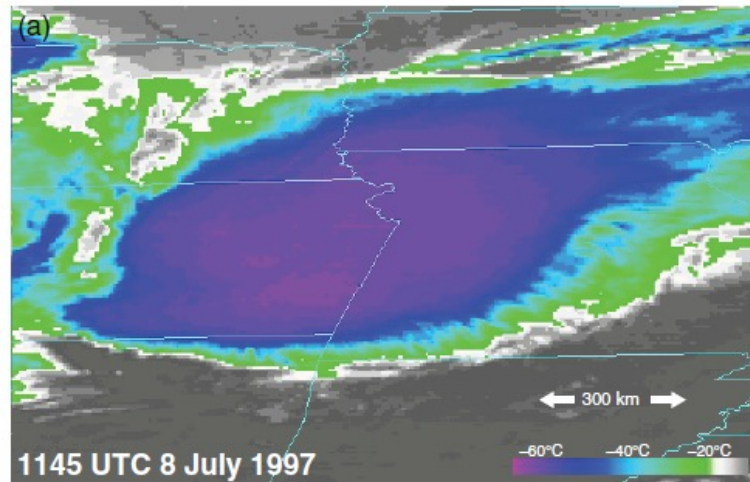


MCV

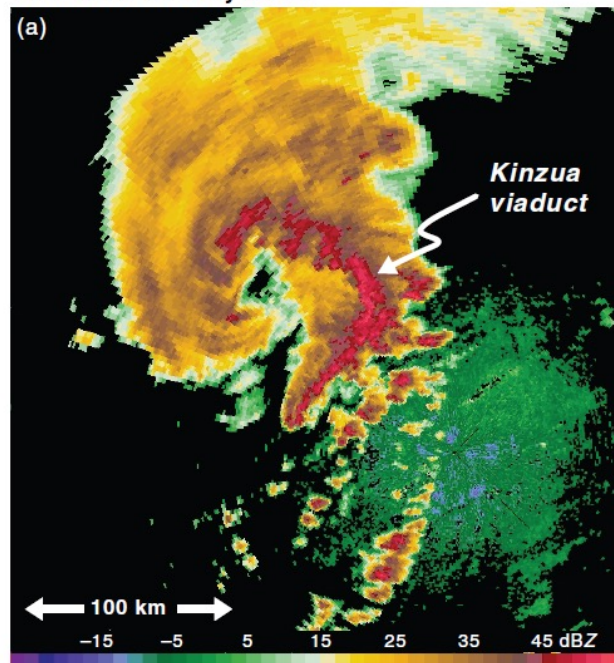


Mesohigh

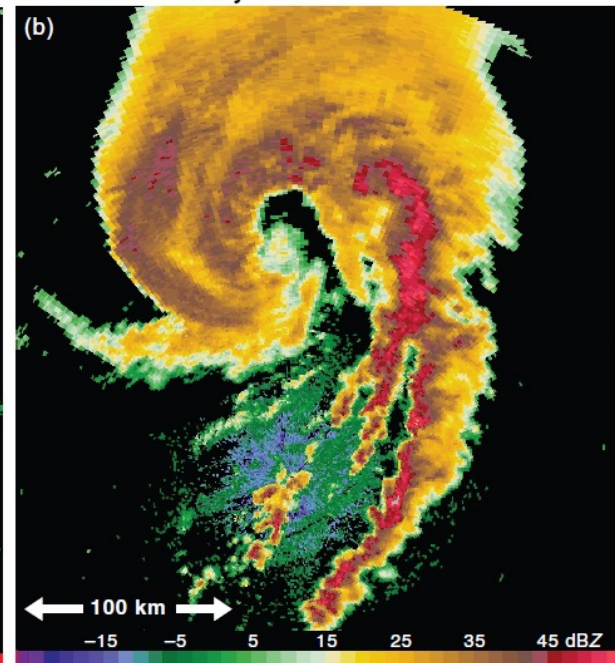
Structure in satellite and radar imageries



1917 UTC 21 July 2003



2032 UTC 21 July 2003



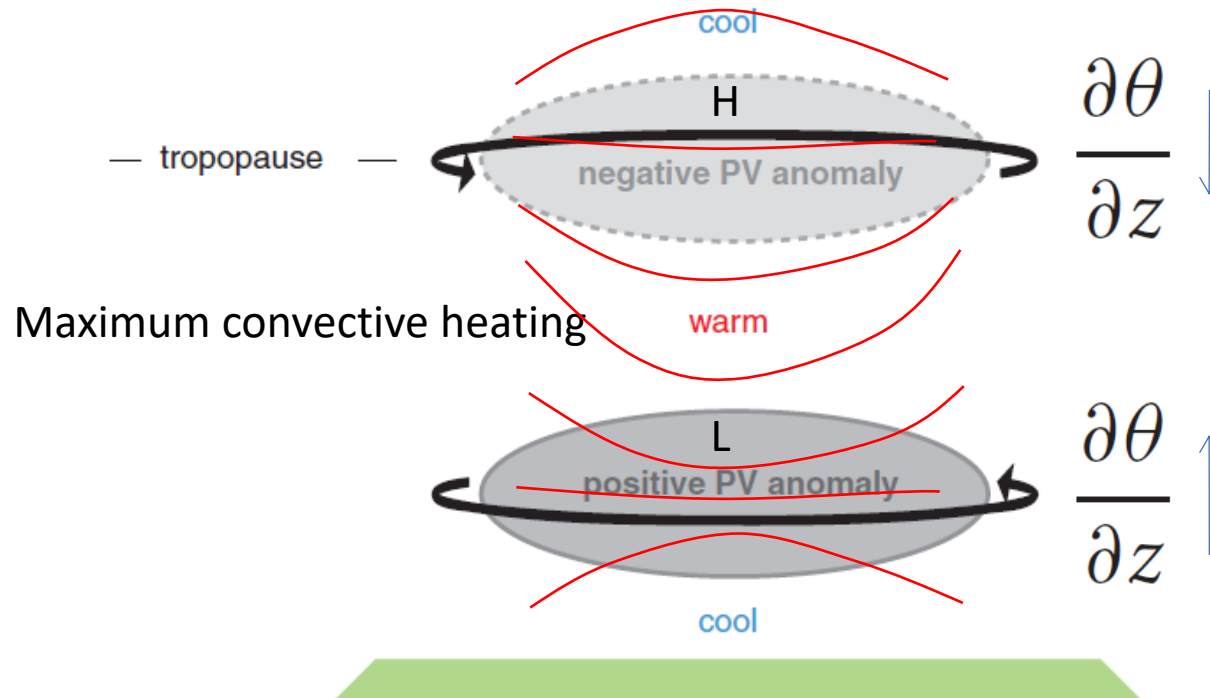
Formation of the cyclonic & anticyclonic circulation

- Potential vorticity anomalies

Ertel PV theorem

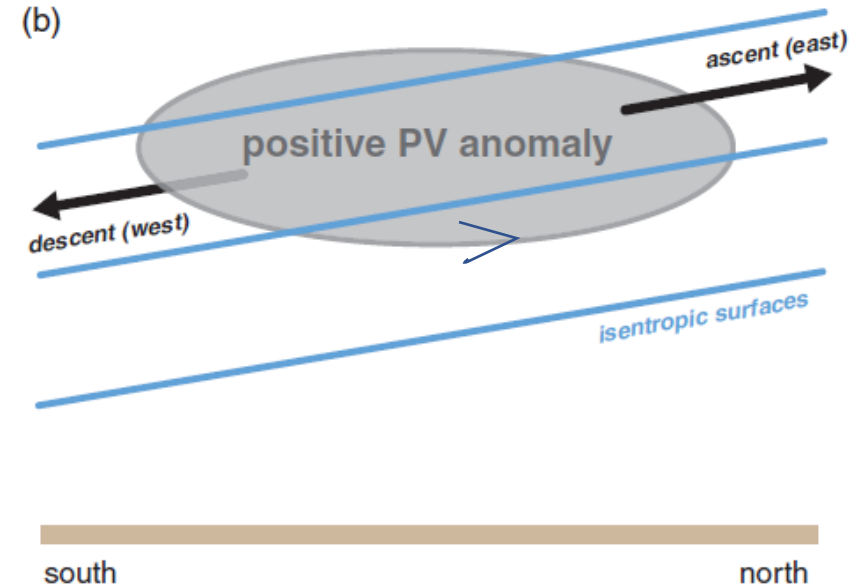
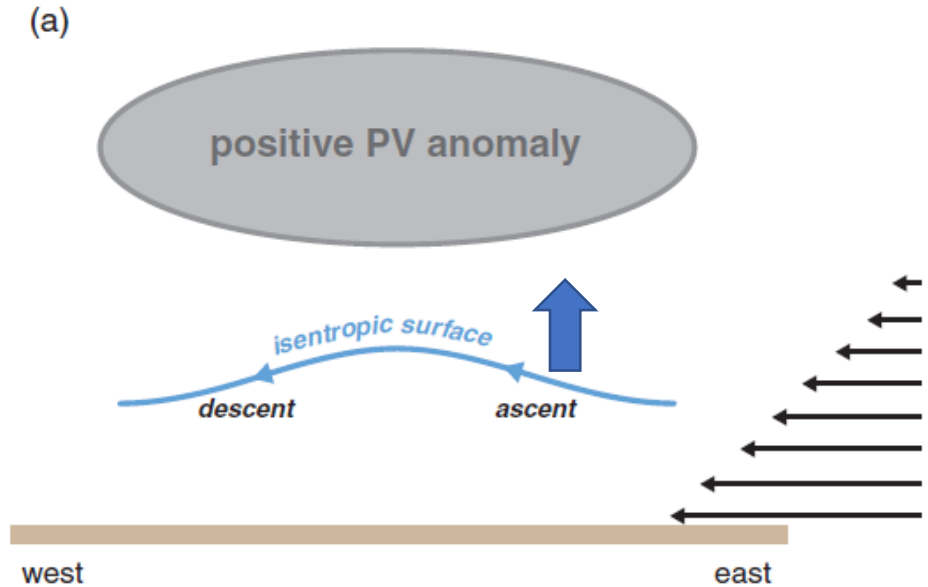
$$\frac{d}{dt} \left\{ \frac{\omega_a \cdot \nabla \lambda}{\rho} \right\} = \frac{\omega_a}{\rho} \cdot \nabla \Psi + \nabla \lambda \cdot \left[\frac{\nabla \rho \times \nabla p}{\rho^3} \right] + \frac{\nabla \lambda}{\rho} \cdot \left\{ \nabla \times \frac{\mathcal{F}}{\rho} \right\}$$

$$PV = \frac{(\boldsymbol{\omega} + f\mathbf{k}) \cdot \nabla \theta}{\rho} \approx \frac{\zeta + f}{\rho} \frac{\partial \theta}{\partial z}$$



Maintenance of MCC

- PV thinking



Vertical shear \rightarrow Thermal Wind \rightarrow tilted isotropic surface

MCV : regeneration of MCS

- MCV may last several days, much longer in time than the MCSs, may survive way beyond its parent MCC
 - It may initiate new convection on the downshear flank
 - The new convection can perpetuate the MCV through latent heat release
- An MCV may turn to be a TC over the ocean